# Pionic Parton Distribution Functions

Florian Linder

Advisor: I. Schienbein

June 11, 2008

# Contents

# Chapter 1

# Introduction

## 1.1 The LPSC – the location of internship

The Laboratoire de Physique Subatomique et de Cosmologie (LPSC) is the institute of fundamental research, where I am doing my internship at the moment. It is situated at the Polygône Scientifique in Grenoble and plays with its about 200 employees a major role in the physics research in France. Additionally, it has numerous scientific collaborations worldwide, amongst others, CERN and Fermilab.

The research is focused on cosmology, such as composition, geometry and evolution of the universe and on particle physics, such as unification of fundamental forces, supersymmetry and quantumchoromo dynamics.

## 1.2 Partons

In this section a basic introduction to the (naive) parton model followed by a description of the modern QCD-improved parton model, derived within the context of quantum chromodynamics (QCD), is provided. For more details we refer to standard textbooks, for example Refs. [1, 2].

The parton model was introduced by Richard Feynman in 1969 as a way to analyze high-energy collisions involving one or two hadrons in the initial state [3]. In the same year, it was applied to electron–proton deep inelastic scattering (DIS) by Bjorken and Paschos [4]. The essence of the parton model is the following assumption: At high energies (in a so called infinite momentum frame), hadrons look like being composed out of point-like and almost free objects called partons. This way, high-energy interactions with initial state hadrons can be described in terms of subprocesses involving pointlike partons. [1] In order to relate the parton level result to the hadron level the flux of incoming partons has to be known, which can be expressed in terms of parton distribution functions (PDFs). The PDF $f_i(\xi)$ is the number density of partons of flavour $i$ carrying a fraction $\xi$ of the parent hadron momentum (or, with other words, $f_i(\xi)\mathrm{d}\xi$ is the number of partons carrying a momentum fraction in the interval $[\xi, \xi + \mathrm{d}\xi]$). Generically, the hadronic cross section $d\sigma$ for a given process can be computed as follows:

$$\mathrm{d}\sigma = \sum_i \int_0^1 \mathrm{d}\xi\, f_i\,(\xi)\,\mathrm{d}\hat{\sigma}_i, \tag{1.1}$$

where an incoherent sum over all partonic subprocesses $\mathrm{d}\hat{\sigma}_i$ is implied. A graphical representation of the parton model for the case of (deep inelastic) electron–pion scattering can be found in Fig. 1.1.

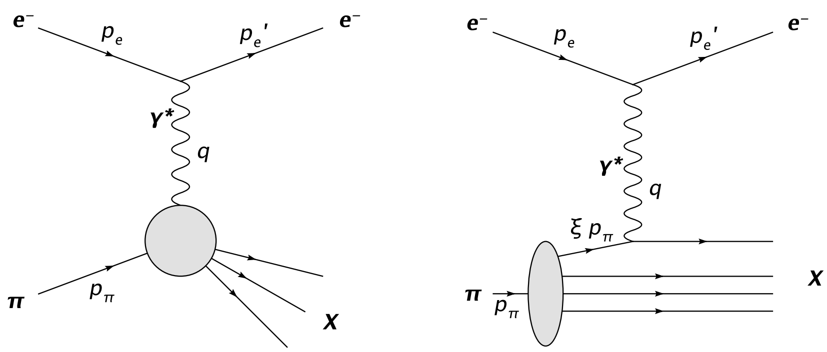


Figure 1.1: Graphical representation of electron–pion scattering. Left: general one-photon exchange diagram. Right: electron–pion scattering in the parton model with electron–parton scattering subprocesses.

In the following years, based on experimental results and the development of QCD it was possible to identify the charged partons with quarks and the neutral ones with gluons. Furthermore, QCD effects were included into the theory leading to the QCD-improved parton model.

The QCD-improved parton model, relying on factorization theorems [5, 6], provides the framework in which almost all cross sections at current high energy colliders are computed and which is also the framework of this work. The factorization theorems state that a large class of physical cross sections can be separated, up to an error which is power-suppressed, into short distance pieces and the PDFs containing the long distance physics. The short

[1] This is a real advantage, since the theoretical description of processes with pointlike objects is much simpler and resembles elementary processes with initial state leptons.

distance parts depend on the process and are calculable order by order in perturbation theory. On the other hand, the PDFs are non-perturbative objects and have to be fixed by experimental information. However, they are universal, i.e., they are the same in all kinds of processes. Therefore, once the PDFs have been determined from a class of measurements they can be used to make predictions for other processes. The general procedure how to extract the PDFs from data will be outlined in the next section. The factorization theorems provide field theoretical definitions of the PDFs as hadronic matrix elements of certain twist-2 operators composed of quark and gluon fields [7]. These definitions are usually not needed in phenomenological analyses of parton distributions. They are, however, necessary to emphasize the field theoretic foundation of the parton model and in order to make contact to nonperturbative models and lattice QCD calculations. QCD corrections lead to the renormalization of these operators such that the PDFs aquire a renormalization scale dependence which is governed by renormalization group equations, the Dokshitzer-Gribov-Lipatov-Altarelli-Parisi (DGLAP) evolution equations [8, 9, 10]. Similar to the short distance coefficients, the DGLAP evolution equations have a perturbative expansion in the strong coupling constant. Recently, the computation of the 3-loop contributions to this expansion (the 3-loop splitting functions) has been completed after several years of effort [11, 12]. With this knowledge it is possible to compute observables at next-to-next-to-leading order (NNLO) accuracy (provided the short distance coefficients are known to this order) allowing for precision tests of perturbative QCD (pQCD). These results are included in the PEGASUS evolution package [13] which will be discussed and used in the next Chap. 2.

The factorized leading twist pQCD formalism described here applies equally to nucleons as well as to pions with the same evolution equations and short distance cross sections irrespective of the target hadron. In the next section, a brief outline will be given, how PDFs are determined from experimental information in so-called 'global analyses of PDFs'. This discussion will be general and applies to any hadron before we turn to pions in Sec. 1.4.

## 1.3 Global analyses of PDFs

Parton distribution functions are determined by performing a global analysis of all available experimental information. It is important to include simultaneously as much of the relevant data as possible for the following reasons. First, different observables are sensitive to different combinations of parton distributions or to distinct kinematic regions such that many data from different processes will better constrain the PDFs. Second, in cases where different processes are sensitive to the same partons the goal is to arrive at a satisfactory description of *all* the data necessitating comprises in the best fit partons. Clearly, leaving out certain data may bias the PDFs towards a specific experiment and furthermore lead to an underestimate of the PDF-uncertainties. It should be noted that such a bias can influence other partons since the partons distributions are coupled to each other by the evolution equations, as will be seen in Chap. 2.

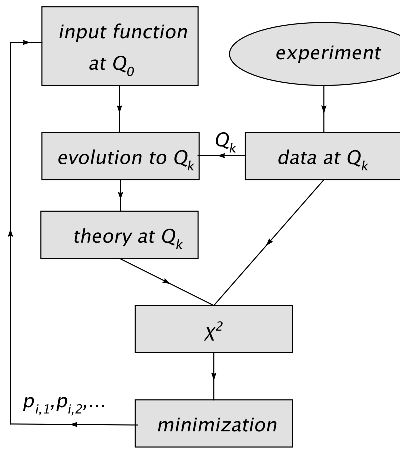


Figure 1.2: Flowchart of a global analysis for parton distribution functions.

The following steps enter a global analysis (see Fig. 1.2):

- First, one chooses suitable input functions $f_i(x, Q_0; p_{i,1}, p_{i,2}, \ldots)$ for the $x$-dependence of the various partons $(i = u, d, s, \ldots, g)$ at some initial scale $Q_0$, where $Q_0$ has to lie in the perturbative regime such that the perturbatively known evolution equations are applicable. Typically, one employs $Q_0 = 1$ or 2 GeV. The fit parameters $p_{i,1}, p_{i,2}, \ldots$ will be optimized during the global analysis. It is important that the functional form of the input distributions has enough flexibility to accommodate the data.

- Then, for each data point $k$, the PDFs are evolved up to the appropriate scale $Q_k$ using the DGLAP evolution equations. Furthermore, the corresponding theory value is computed in the parton model (using the PDFs at the scale $Q_k$ combined with the hard scattering cross sections for the process to which the data point belongs).

- For each data point $k$ the $\chi_k^2$ between the theoretical and the experimental value is calculated. By summing up all $\chi_k^2$ one obtains the

$\chi^2[p_{i,1}, p_{i,2}, \ldots] = \sum_k \chi_k^2$. for a given set of fit parameters $p_{i,1}, p_{i,2}, \ldots$.

- The fit parameters are varied and the procedure is repeated until a global minimum of the $\chi^2$ function is found. The optimal fit parameters finally determine the best-fit PDFs.

## 1.4 A review of pion PDFs

Having outlined the general procedure in the previous section, we now turn to a brief review of global analyses of pion PDFs existing in the literature.

**Owens (1984) [14]** The idea of pionic global analysis came up in 1984 [14] to summarize data from several Drell-Yan (D-Y) experiments of different experimental groups [15, 16, 17, 18]. Unfortunately the D-Y data makes no prediction for momentum fraction $x < 0.2$ which leads to a big ambiguity for small $x$. Another deficit of this pure D-Y data was, that it is neither sensitive to the gluon, nor to the sea distribution. This is due to the fact that the D-Y process is not dominated by gluon and sea diagrams.

**Aurenche** *et al.* **(1989) [19]** To get data which is sensitive to gluon distributions, in 1989, the prompt-photon production was included [19], which is partly dominated by $qg$ scattering. The data here used was taken from $\pi^+p$ or $\pi^-p$ scattering experiments [20, 21]. Like that it was possible to constrain better gluonic pion PDFs. However, the problem of the ambiguity of the sea distribution was not resolved.

In 1991 there were two different approaches [22, 23] using now next-to-leading order (NLO), while the previous pion PDFs [14, 19] were only determined in leading-order (LO) calculations.

**Glück** *et al.* **(1991) [22]** One of those approaches [22] made the reasonable assumption of a valence like parton structure at a low resolution scale $Q^2$, that determines the gluon and sea distribution. Here the experimentally evaluated valence distribution from D-Y data [22] were used. Out of this data, and in combination with the constraints of prompt-photon production [22] to the gluon, one generated sea and valence distribution radiatively.

**Sutton** *et al.* **(1991) [23]** The other approach [23] constrained the valence distribution by D-Y production experiments [23], as well. Thus, the momentum fraction carried by the valence quarks is fixed. But the behavior of the gluon distribution was directly determined by experimental prompt-photon data [24], and the behavior of the sea quark distribution was fixed by quark-counting arguments. Now, to appoint the momentum fraction proportioning between the gluon and sea-quarks, three different plausible assumptions were published. For further comparison I took the middle one where the momentum fraction of the sea input distribution is fixed to 15%.

**Glück** *et al.* **(1998,1999) [25, 26]** In 1997 [25] a new idea came up, namely to constrain the pion PDFs based on nucleonic PDFs using a constituent quark model. This procedure was updated in 1999 [26] with more recent nucleonic input. Here one determined the valence distribution by D-Y data [27, 28, 29]. The obtained valence distribution combined with nucleonic PDFs breed new quark and gluon distributions.

In Fig. 1.3 the PDF parametrisation of the three most recent global analysis [22, 26, 23] at two different input scales are shown. In appendix A the first ten Mellin moments (see Eq. 2.5) at two different scales are listed.

## 1.5 Non-perturbative models and pion PDFs from the lattice

Since about 1980 there exists a numerical approach to QCD, called "lattice QCD simulations". In fact they simulate the QCD field equations in a four-dimensional hyper-cubic space-time lattice. The weakness of this analyzes are the really resource-consuming computational requirements which confine the accuracy. Hence, the most results are not yet very significant. But with increasing speed of current processors and improved simulation techniques this problem will vanish in the near future.

Lattice groups have already constrained regions where global analyzes are vague due to a lack of experimental data, e.g. the small $x$ regions of [30] and gluon [31] distributions. By contrast the behavior of PDFs for big momentum fraction $x$ ($x > 0.7$) could not yet be accurately determined.

In the near future we can expect that the accuracy of those lattice moments is precise enough to constrain the global analysis, as well. Here the pion plays a special role because it has the simplest hadronic structure. Therefore it is chosen to be the first particle whose moments are adequate determined by lattice calculations.

However, there exists some other non perturbative approaches to the pionic structure, as well. E.g. the constituent quark model [32] Nambu-

Jona-Lasinio model [33, 34, 35, 36] and others [37, 38, 39, 40].

## 1.6 Motivation for a new global analysis of pion PDFs

Our goal is to perform a new global analysis of pion PDFs and the present work represents a first step into this direction. In this section we present and discuss several arguments why such a new analysis is interesting despite the fact that there is no new data from pion scattering experiments available.

- As has been discussed in the previous section, pion PDFs are determined from Drell-Yan and prompt photon data obtained in $\pi A$ fixed target experiments. Therefore, the extraction of pion PDFs requires a good knowledge of nuclear PDFs (NPDFs) or nucleon PDFs after nuclear corrections have been applied. Fortunately, much progress has been made on this side of the equation in the past decade. Due to the wealth of new data from the HERA $ep$ collider at DESY and the Tevatron $p\bar{p}$ collider at Fermilab, the proton PDFs are much more precisely known than 10 years ago. Furthermore, methods have been developped in the past few years which allow to determine PDF uncertainties.The nuclear PDFs are still much weaker constrained than the proton PDFs. Nevertheless, there are now sets of NPDFs available which have been determined in NLO QCD [41, 42] where Ref. [42] also includes PDF uncertainties. All this should help, to better determine central pion PDFs along with an analysis of their uncertainties.

- Although there are no new data from pion scattering events available (or expected in the foreseable future), leading neutron data from HERA [43, 44] offer the possibility to constrain the sea quark distribution in the small-$x$ range ($x \simeq 0.01$) [45]. They are therefore complementary to the fixed target Drell-Yan and prompt photon data which lie at larger $x > 0.2$ and it is very interesting to include these data in a global analysis.

- A new technique has been proposed in Ref. [46] how to include the exact NLO cross sections in a fast and efficient way in global analyses of PDFs. This opposed to the standard procedure where a $K$-factor is computed at the beginning of a fit (and possibly updated once in a while) and later the leading order expressions multiplied by the $K$-factor are used in order to compute the theory values in the

$\chi^2$-analysis. As discussed in [46], the $K$-factor method is appropriate when the PDFs are already well-known and just fine-tuned in the following fit. However, pion PDFs are *not* very well known such that an exact computation at NLO seems to be advantageous.

## 1.7 Outline

The rest of this report is organized as follows. In Chap. 2, the necessary steps towards a new global analysis of pion PDFs are described on a more technical level. In the limited time period from April to June it was clearly not possible to deal with all aspects of such an analysis in detail. A large fraction of my time was devoted to studying and testing the Pegasus evolution package such that this part naturally is emphasized. In Chap. 3, the conclusions are drawn and an outlook is given. Tables of Mellin moments of pion PDFs which are useful for comparison with corresponding lattice results are provided in the appendix.

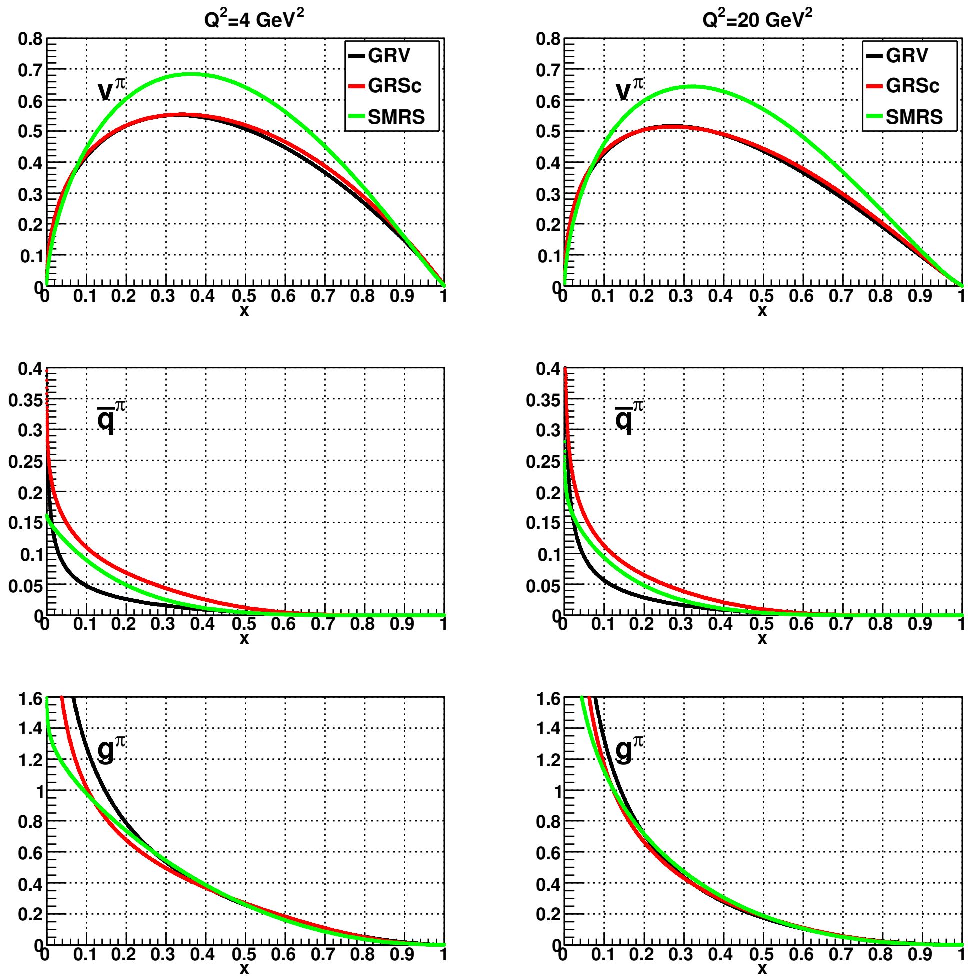


Figure 1.3: Comparison of valence ($v^\pi$), sea ($\bar{q}^\pi$) and gluon ($g^\pi$) distribution in next-to-leading-order of three global analysis: GRV[22], GRSc[26] and SMRS[23]. Left: at input scales $Q^2 = 4$ GeV$^2$, right: at input scale $Q^2 = 20$ GeV$^2$.

# Chapter 2

# Towards a global analysis of pion PDFs

## 2.1 Theoretical Basics

In this section we want to provide some equations and definitions which are used in the following section.

### 2.1.1 Summation rules

Beside the development of the parton model the development of the constituent quark model took place. While the parton model was designed to describe deep inelastic interactions, the constituent quark model was invented to classify the plethora of observed hadrons by introducing a quark substructure.

As we already discussed in Chap.1, charged partons are associated with the quarks of the constituent quark model. But the fact, that PDFs are complicated distributions, shows that this simple static model is not sufficient, it is rather an integration limit of a more complicated dynamic parton theory.

If we integrate over the number density of a quark minus the number density of its antiquark, we find the following relation:

$$\int_0^1 \mathrm{d}\xi \; (f_i(\xi) - f_{\bar{i}}(\xi)) = n_i \; , \tag{2.1}$$

where $n_i \,\epsilon\, \mathbb{N}_0$ is the number of quarks with flavour $i$ of the hadron in the constituent quark model. For the $\pi^+$ we have e.g.:

$$\int_0^1 \mathrm{d}\xi \; (f_i(\xi) - f_{\bar{i}}(\xi)) = \begin{cases} 1 & : \text{ for } i = u \\ 1 & : \text{ for } i = \bar{d} \\ 0 & : \text{ else} \end{cases} \; .$$

Furthermore, the conservation of the momentum of the parent hadron leads us to another important summation rule. By summing over all parton momentum fractions, we should get the momentum of the parent hadron:

$$\sum_{i=u,\bar{u},d,\bar{d},s,\bar{s},\ldots} \int_0^1 \mathrm{d}\xi\, \xi f_i(\xi) = 1. \tag{2.2}$$

### 2.1.2 Valence and sea distribution

To generalize the following definitions of valence and sea distributions for all hadrons, we introduce the $q$-distribution. This is a sum of the PDFs of the quarks which appear in the constituent quark model. The $q$ distribution for the proton is for example $q^p = f_u + f_d$, or for the $\pi^+$ : $q^{\pi^+} = f_u + f_{\bar{d}}$.

With this definition we can define the general valence distribution as $v = q - \bar{q}$, where $\bar{q}$ is called sea (or light sea) distribution.

For the $\pi^+$ we have e.g.: $v^{\pi^+} = (f_u + f_{\bar{d}}) - (f_{\bar{u}} + f_d)$, and $\bar{q}^{\pi^+} = f_{\bar{u}} + f_d$.

### 2.1.3 The QCD-improved parton model

To describe a hadron-hadron scattering process we need to generalize Eq. 1.1 to:

$$\mathrm{d}\sigma = \sum_{i_1,i_2} \int \mathrm{d}\xi_1\, \mathrm{d}\xi_2\, f_{i_1,1}(\xi_1, Q^2)\, f_{i_2,2}(\xi_2, Q^2)\, \mathrm{d}\hat{\sigma}_{\mathrm{i}_1,\mathrm{i}_2}\,, \tag{2.3}$$

where $f_{i,1}(\xi_1, Q^2)$ and $f_{i,2}(\xi_2, Q^2)$ are the PDFs with momentum fraction $\xi_1$ or $\xi_2$ of the two hadrons and $i_1$ and $i_2$ denote the partons.

The data we want to use in our global analysis, Drell-Yan lepton pair and prompt-photon production data, have both been obtained in hadron-hadron scattering processes.

### 2.1.4 Dokshitzer-Gribov-Lipatov-Altarelli-Parisi evolution equations

The $Q^2$ dependency of the parton distributions is described by the Dokshitzer-Gribov-Lipatov-Altarelli-Parisi (DGLAP) evolution equations:

$$\begin{aligned} \frac{\mathrm{d}q_i\,(x,Q^2)}{\mathrm{d}\ln Q^2} &= \frac{\alpha_s}{2\pi}\int_x^1 \frac{\mathrm{d}y}{y}\left[q_i\left(y,Q^2\right)\, P_{qq}\left(\frac{x}{y}\right) + g\left(y,Q^2\right)\, P_{qg}\left(\frac{x}{y}\right)\right], \\ \frac{\mathrm{d}g\,(x,Q^2)}{\mathrm{d}\ln Q^2} &= \frac{\alpha_s}{2\pi}\int_x^1 \frac{\mathrm{d}y}{y}\left[q_i\left(y,Q^2\right)\, P_{gq}\left(\frac{x}{y}\right) + g\left(y,Q^2\right)\, P_{gg}\left(\frac{x}{y}\right)\right]. \end{aligned} \tag{2.4}$$

Where $P_{qq}$ and $P_{qg}$ are the splitting functions which can be calculated perturbatively [11, 12].

### 2.1.5 Mellin space

Now, I want to introduce a useful tool: the Mellin space. PDFs can be either described directly in the $x$-space or in the Mellin moment space. The Mellin $N$ space is defined by the transformation:

$$f(N) = \int_0^1 \mathrm{d}x\, x^{N-1} f(x), N \epsilon\, \mathbb{C}. \tag{2.5}$$

The advantage of changing to this space is that convolution integrals, like in Eq. 2.4, are transformed into simple products. Therefore, in the Mellin-space the evolution equations can be solved analytically. Furthermore, this transformation is quite useful if we want to calculate such integrals on a computer in a very fast and efficient way.

To get back to the $x$-space, the inverse Mellin transform is given by:

$$f(x) = \frac{1}{2\pi i} \int_C \mathrm{d}N\, x^{-N} f(N), \tag{2.6}$$

where C is an arbitrary contour in the complex plane which has to lie right of all singularities and to extend from $-i\infty$ to $i\infty$.

### 2.1.6 Partonic cross sections

In this section, I will describe two QCD mechanisms, which are important for our analyses: The Drell-Yan process and the prompt-photon production. We are going to use mainly experimental data of those two processes in our following analysis.

#### Drell-Yan lepton pair production

The Drell-Yan process is a lepton pair producing quark-antiquark annihilation process (see Fig. 2.1), whose hadronic cross section is composed as in Eq. 2.3.

The partonic cross sections are given by [47]:

$$\frac{\mathrm{d}}{\mathrm{d}M^2} \hat{\sigma}_{q(\xi_1 p_1)\bar{q}(\xi_2 p_2) \to l^+ l^-} = \frac{\sigma_0}{3}\, e_q^2\, \delta(\hat{s} - M^2),$$

where $e_q$ is the quark charge, $\sigma_0 = \frac{4\pi\alpha^2}{3M^3}$ and $\hat{s} = (\xi_1 p_1 + \xi_2 p_2)^2$ the partonic center of mass energy with the momenta of the incoming quarks $\xi_1 p_1$ and $\xi_2 p_2$. Furthermore, $M$ is the invariant mass of the produced lepton pair.

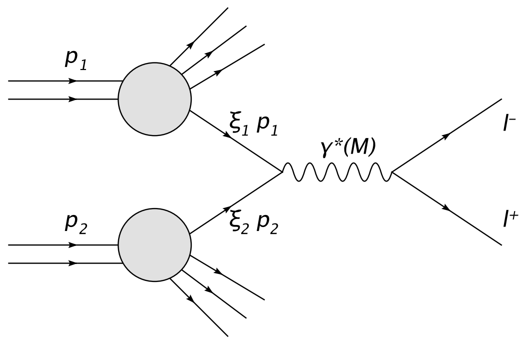


Figure 2.1: Drell-Yan scattering process in the parton model. One sees the splitting up of the two hadrons with momentum $p_1$ and $p_2$ in their partons. The scattering process takes place between the partons with momentum $\xi_1 p_1$ and $\xi_2 p_2$.

### Prompt photon production

In Fig. 2.2 the different leading order Feynman diagrams of the prompt-photon production process are shown: (a) the annihilation process $q\bar{q} \to \gamma g$, and (b) the Compton process $qg \to \gamma q$.

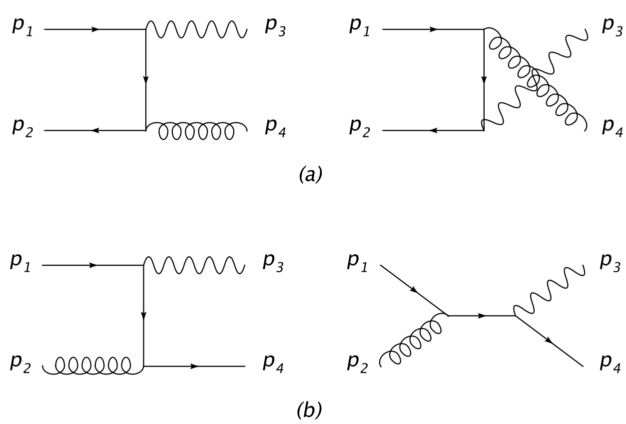


Figure 2.2: Prompt-photon production processes in LO: (a) the two annihilation processes $q\bar{q} \to \gamma g$ and (b) the two Compton processes $qg \to \gamma q$.

The hard cross section for the annihilation process [47] is:

$$\mathrm{d}\hat{\sigma}_{q\bar{q}\to\gamma g} = \frac{4}{9} g^2 e_q^2 \frac{\hat{t}^2 + \hat{u}^2}{\hat{s}\hat{t}\hat{u}} \mathrm{dPS} \; ,$$

and the hard cross section for the Compton process [47] reads:

$$\mathrm{d}\hat{\sigma}_{qg\to\gamma q} = -\frac{1}{6} g^2 e_q^2 \frac{\hat{s}^2 + \hat{u}^2}{\hat{s}^2 \hat{u}} \mathrm{dPS} \ ,$$

where $\hat{s} = (p_1 + p_2)^2 = (p_3 + p_4)^2$, $\hat{u} = (p_1 - p_4)^2 = (p_2 - p_3)^2$ and $\hat{t} = (p_1 - p_3)^2 = (p_2 - p_4)^2$ are the Mandelstam variables of the partons, $e_q$ is the quark charge, $g$ is the strong coupling constant and dPS is the Lorentz invariant phase space.

I want to emphasize here, that we have already gluons appearing in the leading order diagrams. This shows that this process is sensitive to the gluon PDFs and explains the importance of prompt-photon processses in a global analyses to determine the gluonic PDFs.

## 2.2 The PEGASUS package

The QCD-PEGASUS package [13] is a fast and precise program for solving the evolution equations for parton distributions in perturbative QCD. This program contains some thousands of lines written in FORTRAN 77. It has been developed and tested since about 1990 and its predecessors had been used for important publications on PDFs [48, 26]. It is rather modularly programmed and quite well documented, thus relatively easy to use.

The differential equations are solved in the Mellin-space, which drastically improves the speed of the computational simulations. Additionally it is able to evaluate unpolarized PDFs in the $\overline{MS}$ renormalization scheme up to next-to-next-to-leading order, where one can choose also between different heavy flavours scheme. A lot of other different configurations are possible: e.g. different fast Mellin inversions and various evolution modes beyond leading order.

The reason why we have chosen this package for our purposes is not only the fact that it is well written, nor only the beauty of the solution in the Mellin space, the primary reason is its fast simulation speed. This high speed is quite important for our algorithm to determine the pion PDFs: We have to repeat the loop, shown in the flow chart in Fig. 1.2, quite often. Thus we can avoid immense simulation times. On the other hand one disadvantage is that one has to know the hard cross sections of section 2.1.6 in the Mellin space to connect theory and experimental data.

### 2.2.1 Description

The PEGASUS package works as follows:

- First, the input PDFs are transformed from the momentum $x$-space to the Mellin $N$ space (see Eq. 2.5) at certain support points $N$.
- Then, the evolution in the Mellin space takes place where it should be noted that different moments evolve independently
- To obtain the evolved PDFs in $x$-space, a Mellin inversion is necessary (see Eq. 2.6). This inverse transform is unfortunately not possible to be solved analytically. So an approximative integration on a contour in the complex Mellin space is used. For this integration it is necessary to have the Mellin moments at various support points on the integration contour. Exactly these Mellin moments had to be determined and evolved before.

**Input function**

We use with the PEGASUS package the following parametrization for our input functions:

$$x f_i(x, Q_0^2) = N_i \, p_{i,1} \, x^{p_{i,2}} (1-x)^{p_{i,3}} \left[1 + p_{i,5} x^{p_{i,4}} + p_{i,6} x\right], \tag{2.7}$$

where $f_i(x, Q_0^2)$ are gluon and quark PDFs in the momentum $x$-space. In this functional form we have 7 parameters $(N_i, p_{i,1} - p_{i,6})$ for each distribution. However, not all of them are free: the summation rules in Eqs. 2.1 and 2.2 discussed previously give three additional constraints.

As we already mentioned, only a finite number of support points in the complex plain is necessary for an accurate Mellin inversion. The fact that the complicated convolution integrals in $x$-space turn into ordinary products in Mellin $N$-space helps a lot. Thus, only the Mellin moments at those support points $N$ need to be known to finally obtain the evolved parton distribution in the $x$-space.

The analytic form of the Mellin transform of our input parametrization (Eq. 2.7) can be written as follows:

$$\begin{aligned} f_i(N, Q_0^2) = & N_i \, p_{i,1} (B(N + p_{i,2} - 1, \; p_{i,3} + 1) \\ & + p_{i,5} B(N + p_{i,2} + p_{i,4} - 1, \; p_{i,3} + 1) \\ & + p_{i,6} B(N + p_{i,2}, \; p_{i,3} + 1)) \; , \end{aligned}$$

where $B(x, y)$ is the Euler-beta-function.

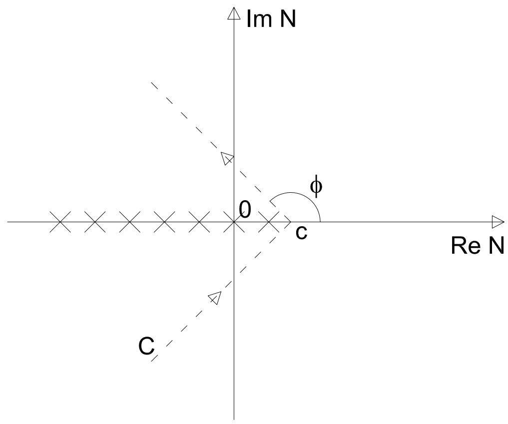


Figure 2.3: The contour in the complex plain for the Mellin inversion integral used in the PEGASUS package.

### Mellin inversion

In Fig. 2.3 one can see the form of the contour of the Mellin inversion integral. This contour, $C = c + ze^{i\phi}$ $(z\epsilon[0, 80])$, has been optimized in the PEGASUS package for nucleonic PDFs with parameters $c = \frac{3}{4}\pi$ and $\phi = 1.9$. The integral on this contour is performed as several eight-point Gauss-Legendre integrations [49]. All in all, there are 144 Points used to solve the inversion (in the more accurate mode with IFAST = 0).

## 2.2.2 Modifications and tests

As already mentioned, the PEGASUS package is originally designed for proton PDFs. To use it for the pion, I had to program and test pionic boundary conditions for the DGLAP differential equations.

### New input function

For the input, the PEGASUS package uses not the direct parametrization of the particular partons ($u$, $\bar{u}$, $d$, $\bar{d}$, ... , $g$), but it uses some linear combinations of them. However, those linear combinations are designed for hadrons containing $u$ and $d$ quarks in the valence structure, e.g. protons or neutrons. Pions, which consists, amongst others, of $\bar{u}$ $(\pi^-)$ and $\bar{d}$ $(\pi^+)$ quarks in the valence structure are not really respected.

I generalized those parametrizations in a new input function by interpreting the $u$ distribution as $q_1$, the $d$ distribution as $q_2$ and the strange distribution as $q_3$. This works because the evolution equations are similar for all quarks and so the different quark distributions can be handled equally, i.e. in the case of the $\pi^+$: $q_1$ equates to $u$ and $q_2$ equates to $\bar{d}$.

The only aspect we have to take into account is, that the $q_3$ distribution must not appear as valence quark of the hadron. That's why one can only handle hadrons with two different types of valence quarks with this package.

By parameterizing the input functions, we have to respect one point: The fact, that not all parameters of our parametrization are free (this is explained by the summation rules of Eqs. 2.1 and 2.2) would lead to an over-determination of the distribution, if we give all parameters. Thus the parameters $p_{1,q_1}$ and $p_{1,q_2}$ are the number of valence quarks in the constituent quark model, and the parameter $p_{1,g}$ is always equal one.

### Tests with recent pionic PDFs

To test my rewritten input function and parametrization, I used two recent parameterizations of global PDFs [23, 26].

**Mellin transformation** First, I tested the parametrization of the pionic input PDFs. I transformed this input in Mellin moments on the integration

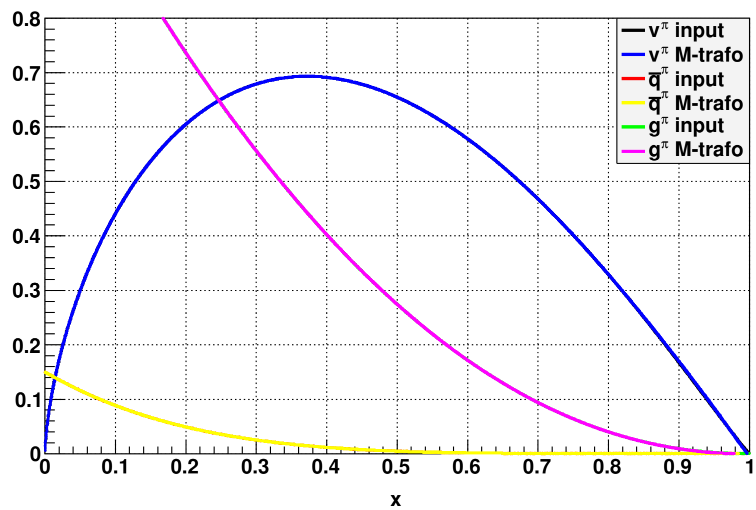


Figure 2.4: Comparison of the Mellin-transformed and inverse-Mellin-transformed NLO parton distributions (M-trafo) at the input scale $Q^2 = 4\ \mathrm{GeV}^2$ with the original parametrization (input) of Sutton *et al.* [23].

contour. Then I made the approximate inverse Mellin transform with these support points without any evolution. In Fig. 2.4 the transformed and re-transformed pionic parton distributions of Sutton *et al.* [23] are compared with the original parametrization. Here, we see that the two functions agree perfectly well. In fact the corresponding curves are on top of each other.

In Fig. 2.5 we see the same procedure for the parton distributions of Glück *et al.* [26]. In this case the distributions at large $x$ show a visible difference.

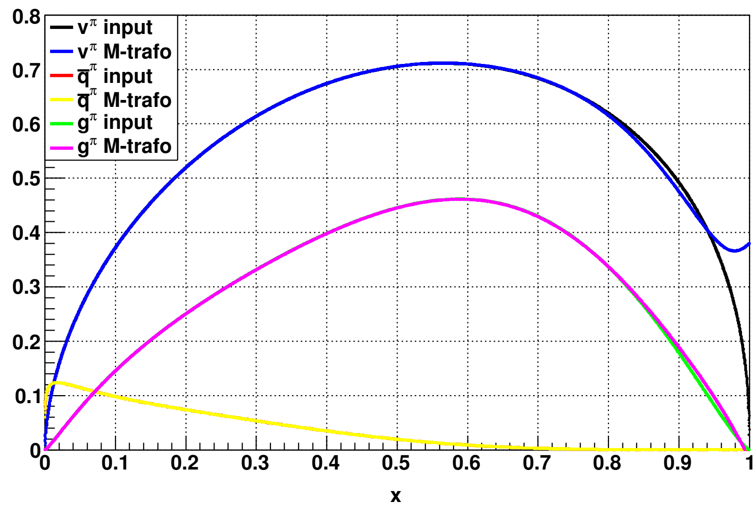


Figure 2.5: Comparison of the Mellin-transformed and inverse-Mellin-transformed NLO parton distributions (M-trafo) at the input scale $Q^2 = 0.4$ GeV$^2$ with the original parametrization (input) of Glück *et al.* [26].

This can only be caused by the inverse Mellin transformation. I checked, with some Mellin moments (at $N = 1, 2, .., 10, 99, 100$), the equivalence of the moments determined by the PEGASUS package with the moments directly integrated with Mathematica. The variation was negligible ($\frac{\Delta v^\pi}{v^\pi} < 0.005$), thus one can assume that the difference between the two curves in Fig. 2.5 is caused by the inverse Mellin transform.

In the parton distributions by Glück *et al.* [26] the parameter $p_3$ of the valence distribution is remarkably small in comparison with the parametrization of Sutton *et al.* [23] or proton PDFs [48]. By varying this parameter, we determined that for the values of $p_3 < 1$ the inversion is inaccurate at large $x > 0.95$, wheras for $p_3 > 1$ the Mellin inversion always converged to the used input function.

To solve this problem, I tried to vary the parameters of the Mellin inversion $c$ and $\phi$ and I programmed a new mode (IFAST $= -1$), which uses more points on a longer contour for the Mellin inversion to improve this defect. None of these simple solutions worked very well. However, it is not a principal convergence problem of the Mellin-inversion. The chosen PDF parametrization should converge generally.

The next step would be to optimize the approximative Mellin inversion e.g. like in Refs. [50, 51]. However, we can assume that this special case does not appear. On the one hand, other pion [23] and proton distributions [48] have a parameter $p_3 > 1$. Moreother, nonperturbative QCD calculations such as Dyson-Schwinger equation models [52, 53] predict that $p_3 \simeq 2$. If, we finally obtain $p_3$ which is really smaller than 1 we should solve this problem. But if $p_3$ stays greater than 1, we do not have to care about it.

**Evolution** The next step was to test the evolution of the PEGASUS package. For this test I took the PDFs of Glück *et al.* [26]. I compared the PEGASUS evolved input PDFs with those of the FORTRAN parametrization package provided by Glück *et al.* [26]. For the evolution I took the same parameters like in the publication: fixed flavour number scheme (IVFNS $=$ 0) with three flavours (NFF $= 3$), the standard evolution mode (IMODE $=$ 1), the NLO pertubative mode (NPORD $= 1$) and a constant ratio of the factorization and renormalization scale (FR2 $= 1$). For the input scale I took $Q_0^2 = 0.4$ GeV$^2$), for the strong coupling constant $a_s = \frac{\alpha_s}{4\pi} = 0.5779$ and for the charm quark mass $m_c^2 = 2.0$ GeV$^2$.

In Fig. 2.6 those distributions are compared at two different scales: $Q^2 =$ 4 GeV$^2$ and $Q^2 = 1000$ GeV$^2$. One can see that these two agree quite well and that the evolution works!

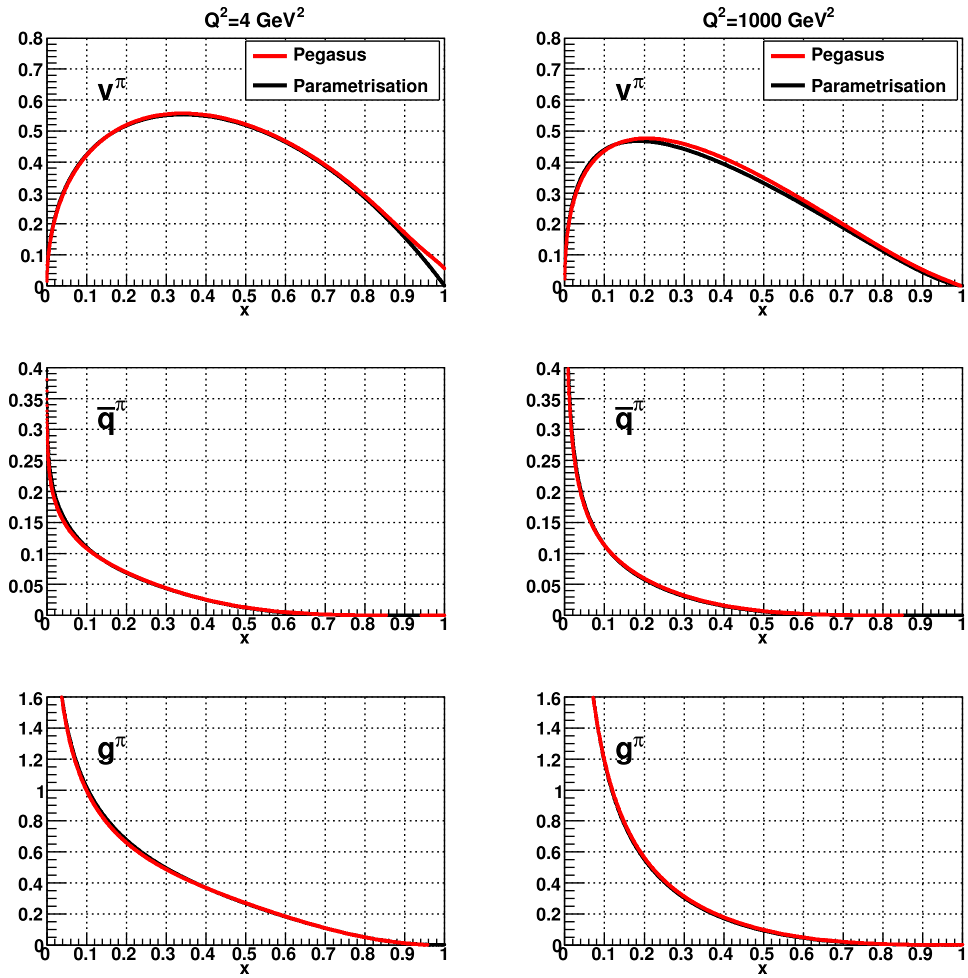


Figure 2.6: Comparison of the NLO parton distributions generated by the parametrization package provided by Glück *et al.* [26] with the evolved parton distributions by the PEGASUS package. Left: at input scales $Q^2 = 4\ \mathrm{GeV}^2$, right: at input scale $Q^2 = 1000\ \mathrm{GeV}^2$.

# Chapter 3

# Conclusions and Outlook

In this work I have first described the naive parton model, followed by the QCD-improved parton model. This is relying on the QCD factorization-theorems. It defines well the PDFs from a field-theoretical point of view, which is necessary to compare parton model results with Lattice QCD and other non-perturbative theories. Then I sketched the functionality of a global analysis. The preparation of such a global analysis was the aim of this study. The report continues with a review of literature concerning pionic structure, where I emphasized the literature related to global analyses. This is followed by some theoretical background which we needed for the QCD-PEGASUS package and which is described afterwards. This package is a program to evolve parton distributions with the DGLAP evolution equations up to NNLO. For the procedure of determining a global analysis this is one of the basic ingredients. Finally I implemented boundary conditions for pion PDFs into the PEGASUS package and tested them extensively.

Now, the following steps remain to be done:

- To evaluate the theory of the cross sections in higher order in the Mellin-space.
- To include experimental data of Drell-Yan, prompt-photon processes and also leading neutron data from HERA.
- To interface a minimizing package, such as Minuit to our code, and to include a method (Hessian method or Lagrange multipliers method) to determine PDF uncertainties.

Beside the physics I learned simultaneously a lot utilities for a physicist: On the one hand, I read a lot of scientific papers, which was at the beginning quite hard; but after having read various papers, I got used to the style of scientific literature and I learned how to extract important information for me. On the other hand, I learned to use a lot of computational tools, such as programming in FORTRAN, writing Makefiles, using debugging and version control utilities and finally using the royal plot program Root.

At this point, I want to thank my advisor, Ingo Schienbein, that he supported me in all my interests of study, regardless of the type and that he was always patient to answer all my questions.

# Appendix A

# Mellin moments

| $N$ | PDF | $\mathrm{SMRS}_\pi$ [23] | $\mathrm{GRV}_\pi$ [22] | $\mathrm{GRSc}_\pi$ [26] |
|---|---|---|---|---|
| | $v^\pi$ | 0.998 | 0.992 | 0.998 |
| 1 | $\bar{q}^\pi$ | 1.46 | 4.27 | 3.56 |
| | $g^\pi$ | 15.0 | 84.0 | 58.3 |
| | $v^\pi$ | 0.231 | 0.194 | 0.198 |
| 2 | $\bar{q}^\pi$ | 0.0253 | 0.0178 | 0.0369 |
| | $g^\pi$ | 0.384 | 0.511 | 0.433 |
| | $v^\pi$ | 0.101 | 0.0832 | 0.0862 |
| 3 | $\bar{q}^\pi$ | 0.00357 | 0.00242 | 0.00598 |
| | $g^\pi$ | 0.0895 | 0.0978 | 0.0920 |
| | $v^\pi$ | 0.0560 | 0.0465 | 0.0486 |
| 4 | $\bar{q}^\pi$ | 0.000888 | 0.000706 | 0.00174 |
| | $g^\pi$ | 0.0344 | 0.0374 | 0.0367 |
| | $v^\pi$ | 0.0354 | 0.0298 | 0.0313 |
| 5 | $\bar{q}^\pi$ | 0.000296 | 0.000280 | 0.000655 |
| | $g^\pi$ | 0.0167 | 0.0188 | 0.0186 |
| | $v^\pi$ | 0.0244 | 0.0208 | 0.0219 |
| 6 | $\bar{q}^\pi$ | 0.000118 | 0.000132 | 0.000289 |
| | $g^\pi$ | 0.00930 | 0.0110 | 0.0108 |
| | $v^\pi$ | 0.0177 | 0.0153 | 0.0162 |
| 7 | $\bar{q}^\pi$ | 5.38E-05 | 7.00E-05 | 0.000142 |
| | $g^\pi$ | 0.00569 | 0.00703 | 0.00685 |
| | $v^\pi$ | 0.0135 | 0.0118 | 0.0125 |
| 8 | $\bar{q}^\pi$ | 2.70E-05 | 4.03E-05 | 7.51E-05 |
| | $g^\pi$ | 0.00373 | 0.00481 | 0.00460 |
| | $v^\pi$ | 0.0106 | 0.00879 | 0.00932 |
| 9 | $\bar{q}^\pi$ | 1.45E-05 | 2.39E-05 | 4.05E-05 |
| | $g^\pi$ | 0.00257 | 0.00307 | 0.00288 |
| | $v^\pi$ | 0.00849 | 0.00713 | 0.00756 |
| 10 | $\bar{q}^\pi$ | 8.27E-06 | 1.53E-05 | 2.40E-05 |
| | $g^\pi$ | 0.00185 | 0.00228 | 0.00209 |

Table A.1: $Q^2 = 4$ GeV$^2$ Mellin moments NLO bla

Table A.2: Comparison of valence ($v^\pi$), sea ($\bar{q}^\pi$) and gluon ($g^\pi$) NLO Mellin moments of three global analysis: GRV[22], GRSc[26] and SMRS[23] at input scales $Q^2 = 4$ GeV$^2$.

| $N$ | PDF | SMRS$_\pi$ [23] | GRV$_\pi$ [22] | GRSc$_\pi$ [26] |
|---|---|---|---|---|
| | $v^\pi$ | 0.998 | 0.990 | 0.997 |
| 1 | $\bar{q}^\pi$ | 2.18 | 7.16 | 6.02 |
| | $g^\pi$ | 44.2 | 157 | 125 |
| | $v^\pi$ | 0.210 | 0.171 | 0.174 |
| 2 | $\bar{q}^\pi$ | 0.0266 | 0.0214 | 0.0376 |
| | $g^\pi$ | 0.408 | 0.518 | 0.468 |
| | $v^\pi$ | 0.0868 | 0.0685 | 0.0703 |
| 3 | $\bar{q}^\pi$ | 0.00351 | 0.00252 | 0.00541 |
| | $g^\pi$ | 0.0748 | 0.0760 | 0.0738 |
| | $v^\pi$ | 0.0465 | 0.0365 | 0.0377 |
| 4 | $\bar{q}^\pi$ | 0.000848 | 0.000681 | 0.00148 |
| | $g^\pi$ | 0.0255 | 0.0252 | 0.0253 |
| | $v^\pi$ | 0.0286 | 0.0225 | 0.0234 |
| 5 | $\bar{q}^\pi$ | 0.000278 | 0.000255 | 0.000537 |
| | $g^\pi$ | 0.011443 | 0.011513 | 0.011578 |
| | $v^\pi$ | 0.0192 | 0.0152 | 0.0159 |
| 6 | $\bar{q}^\pi$ | 0.000110 | 0.000115 | 0.000230 |
| | $g^\pi$ | 0.00601 | 0.00623 | 0.00622 |
| | $v^\pi$ | 0.0137 | 0.0110 | 0.0114 |
| 7 | $\bar{q}^\pi$ | 4.97E-05 | 5.89E-05 | 0.000110 |
| | $g^\pi$ | 0.00350 | 0.00376 | 0.00369 |
| | $v^\pi$ | 0.0102 | 0.00824 | 0.00861 |
| 8 | $\bar{q}^\pi$ | 2.48E-05 | 3.28E-05 | 5.71E-05 |
| | $g^\pi$ | 0.00220 | 0.00244 | 0.00235 |
| | $v^\pi$ | 0.00790 | 0.00642 | 0.00671 |
| 9 | $\bar{q}^\pi$ | 1.34E-05 | 1.95E-05 | 3.17E-05 |
| | $g^\pi$ | 0.00146 | 0.00168 | 0.00158 |
| | $v^\pi$ | 0.00626 | 0.00513 | 0.00536 |
| 10 | $\bar{q}^\pi$ | 7.64E-06 | 1.22E-05 | 1.85E-05 |
| | $g^\pi$ | 0.00102 | 0.00120 | 0.00110 |

Table A.3: Comparison of valence ($v^\pi$), sea ($\bar{q}^\pi$) and gluon ($g^\pi$) NLO Mellin moments of three global analysis: GRV[22], GRSc[26] and SMRS[23] at input scales $Q^2 = 20$ GeV$^2$.

# Bibliography


[1] F. Halzen and A. D. Martin, *Quarks and Leptons.* John Wiley and Sons, 1985.

[2] E. Leader and E. Predazzi, *An introduction to gauge theories and modern particle physics, Volume 1 and 2.* Cambridge University Press, 1996.

[3] R. P. Feynman. In *Proceedings of the 3rd Topical Conference on High Energy Collisions of Hadrons*, Stonybrook, NY, 1969, ed. C. N. Yang *et al.*, p. 237. New York: Gordon and Breach.

[4] J. D. Bjorken and E. A. Paschos, *Inelastic Electron Proton and gamma Proton Scattering, and the Structure of the Nucleon*, *Phys. Rev.* **185** (1969) 1975–1982.

[5] J. C. Collins, D. E. Soper, and G. Sterman, *Factorization of Hard Processes in QCD*, *Adv. Ser. Direct. High Energy Phys.* **5** (1988) 1–91, [`hep-ph/0409313`].

[6] J. C. Collins and D. E. Soper, *The Theorems of perturbative QCD*, *Ann. Rev. Nucl. Part. Sci.* **37** (1987) 383.

[7] J. C. Collins and D. E. Soper, *Parton Distribution and Decay Functions*, *Nucl. Phys.* **B194** (1982) 445.

[8] V. N. Gribov and L. N. Lipatov, *Deep inelastic ep scattering in perturbation theory*, *Sov. J. Nucl. Phys.* **15** (1972) 438–450.

[9] G. Altarelli and G. Parisi, *Asymptotic Freedom in Parton Language*, *Nucl. Phys.* **B126** (1977) 298.

[10] Y. L. Dokshitzer, *Calculation of the Structure Functions for Deep Inelastic Scattering and $e^+e^-$ Annihilation by Perturbation Theory in Quantum Chromodynamics (In Russian)*, *Sov. Phys. JETP* **46** (1977) 641–653.

[11] S. Moch, J. A. M. Vermaseren, and A. Vogt, *The three-loop splitting functions in QCD: The non-singlet case*, *Nucl. Phys.* **B688** (2004) 101–134, [hep-ph/0403192].

[12] A. Vogt, S. Moch, and J. A. M. Vermaseren, *The three-loop splitting functions in QCD: The singlet case*, *Nucl. Phys.* **B691** (2004) 129–181, [hep-ph/0404111].

[13] A. Vogt, *Efficient evolution of unpolarized and polarized parton distributions with QCD-PEGASUS*, *Comput. Phys. Commun.* **170** (2005) 65–92, [hep-ph/0408244].

[14] J. F. Owens, *$Q^2$ Dependent Parametrizations of Pion Parton Distribution Functions*, *Phys. Rev.* **D30** (1984) 943.

[15] **NA3** Collaboration, J. Badier *et. al.*, *Experimental $J/\psi$ Hadronic Production from 150-GeV/c to 280-GeV/c*, *Z. Phys.* **C20** (1983) 101.

[16] M. J. Corden *et. al.*, *Experimental Comparison of $J/\psi$ Production by $pi^{+-}$, $K^{+-}$, $p$ and $\bar{p}$ Beams at 39.5-GeV/c*, *Phys. Lett.* **B68** (1977) 96.

[17] E. Anassontzis *et. al.*, *Production of muon pairs with masses greater than 4- GeV/$c^2$ in $\bar{p}n$ and $\pi^- n$ interactions at 125- GeV/c*, . Presented at 21st Int. Conf. on High Energy Physics, Paris, France, Jul 26-31, 1982.

[18] **NA3** Collaboration, P. Mine, *Muon pair production ($M > 4.1$ $(GeV/c)^2$) by $\pi^-$ at 150 (GeV/c), 200 (GeV/c) and 280 (GeV/c) in the Cern NA3 experiment. (talk)*, . In *Madison 1980, Proceedings, High Energy Physics-1980, Part 1*, 147-148.

[19] P. Aurenche, R. Baier, M. Fontannaz, M. N. Kienzle-Focacci, and M. Werlen, *The gluon content of the pion from high $p_T$ direct photon production*, *Phys. Lett.* **B233** (1989) 517.

[20] **WA70** Collaboration, M. Bonesini *et. al.*, *Production of High Transverse Momentum Prompt Photons and Neutral Pions in Proton Proton Interactions at 280-GeV/c*, *Z. Phys.* **C38** (1988) 371.

[21] **NA24** Collaboration, C. De Marzo *et. al.*, *A measurement of $\pi^0$ production at large transverse momentum in $\pi^- p$, $\pi^+ p$ and $pp$ collision at 300-GeV/c*, *Phys. Rev.* **D36** (1987) 16.

[22] M. Gluck, E. Reya, and A. Vogt, *Pionic parton distributions*, *Z. Phys.* **C53** (1992) 651–656.

[23] P. J. Sutton, A. D. Martin, R. G. Roberts, and W. J. Stirling, *Parton distributions for the pion extracted from Drell-Yan and prompt photon experiments*, *Phys. Rev.* **D45** (1992) 2349–2359.

[24] **WA70** Collaboration, M. Bonesini *et. al.*, *high transverse momentum prompt photon production by $\pi^-$ and $\pi^+$ on protons at 280-GeV/c*, *Z. Phys.* **C37** (1988) 535.

[25] M. Gluck, E. Reya, and M. Stratmann, *Mesonic parton densities derived from constituent quark model constraints*, *Eur. Phys. J.* **C2** (1998) 159–163, [hep-ph/9711369].

[26] M. Gluck, E. Reya, and I. Schienbein, *Pionic parton distributions revisited*, *Eur. Phys. J.* **C10** (1999) 313–317, [hep-ph/9903288].

[27] **NA10** Collaboration, B. Betev *et. al.*, *Differential cross-section of high mass muon pairs produced by a* 194 (GeV/c) $\pi^-$ *beam on a tungsten target*, *Z. Phys.* **C28** (1985) 9.

[28] **NA10** Collaboration, P. Bordalo *et. al.*, *nuclear effects on the nuclear structure functions in hadronic high mass dimuon production*, *Phys. Lett.* **B193** (1987) 368.

[29] J. S. Conway *et. al.*, *Experimental Study of Muon Pairs Produced by 252-GeV Pions on Tungsten*, *Phys. Rev.* **D39** (1989) 92–122.

[30] W. Detmold, W. Melnitchouk, and A. W. Thomas, *Parton distribution functions in the pion from lattice QCD*, *Phys. Rev.* **D68** (2003) 034025, [hep-lat/0303015].

[31] H. B. Meyer and J. W. Negele, *The Glue Content of the Pion*, *PoS* **LATTICE2007** (2006) 154, [0710.0019].

[32] G. Altarelli, S. Petrarca, and F. Rapuano, *The Pion Structure Function in a Constituent Model*, *Phys. Lett.* **B373** (1996) 200–206, [hep-ph/9510346].

[33] W. Bentz, T. Hama, T. Matsuki, and K. Yazaki, *NJL model on the light cone and pion structure function*, *Nucl. Phys.* **A651** (1999) 143–173, [hep-ph/9901377].

[34] T. Shigetani, K. Suzuki, and H. Toki, *Pion structure function in the Nambu and Jona-Lasinio model*, *Phys. Lett.* **B308** (1993) 383–388, [hep-ph/9402286].

[35] R. M. Davidson and E. Ruiz Arriola, *Parton distributions functions of pion, kaon and eta pseudoscalar mesons in the NJL model*, *Acta Phys. Polon.* **B33** (2002) 1791–1808, [hep-ph/0110291].

[36] E. Ruiz Arriola and W. Broniowski, *Pion light-cone wave function and pion distribution amplitude in the Nambu-Jona-Lasinio model*, *Phys. Rev.* **D66** (2002) 094016, [hep-ph/0207266].

[37] A. E. Dorokhov and L. Tomio, *Pion structure function within the instanton model*, *Phys. Rev.* **D62** (2000) 014016.

[38] F. Bissey *et. al.*, *A model for the pion structure function*, *Phys. Lett.* **B547** (2002) 210–218, [hep-ph/0207107].

[39] T. Frederico and G. A. Miller, *Deep inelastic structure function of the pion in the null plane phenomenology*, *Phys. Rev.* **D50** (1994) 210–216.

[40] W. Melnitchouk, *Quark hadron duality in electron pion scattering*, *Eur. Phys. J.* **A17** (2003) 223–234, [hep-ph/0208258].

[41] D. de Florian and R. Sassot, *Nuclear parton distributions at next-to-leading order*, *Phys. Rev.* **D69** (2004) 074028, [hep-ph/0311227].

[42] M. Hirai, S. Kumano, and T. H. Nagai, *Determination of nuclear parton distribution functions and their uncertainties at next-to-leading order*, *Phys. Rev.* **C76** (2007) 065207, [0709.3038].

[43] **H1** Collaboration, C. Adloff *et. al.*, *Measurement of leading proton and neutron production in deep inelastic scattering at HERA*, *Eur. Phys. J.* **C6** (1999) 587–602, [hep-ex/9811013].

[44] **ZEUS** Collaboration, S. Chekanov *et. al.*, *Leading neutron production in e+ p collisions at HERA*, *Nucl. Phys.* **B637** (2002) 3–56, [hep-ex/0205076].

[45] M. Klasen, *The pion structure function and jet production in* $\gamma p \to nX$, *J. Phys.* **G28** (2002) 1091–1102, [hep-ph/0107011].

[46] M. Stratmann and W. Vogelsang, *Towards a global analysis of polarized parton distributions*, *Phys. Rev.* **D64** (2001) 114007, [hep-ph/0107064].

[47] R. K. Ellis, W. J. Stirling, and B. Webber, *QCD and Collider Physics.* Cambridge University Press, 1996.

[48] M. Gluck, E. Reya, and A. Vogt, *Dynamical parton distributions revisited*, *Eur. Phys. J.* **C5** (1998) 461–470, [hep-ph/9806404].

[49] M. Abramowitz and I. A. Stegun, *Handbook of Mathematical Functions with Formulas, Graphs, and Mathematical Tables.* Dover, New York, ninth dover printing, tenth gpo printing ed., 1964.

[50] D. A. Kosower, *Evolution of parton distributions*, *Nucl. Phys.* **B506** (1997) 439–467, [hep-ph/9706213].

[51] S. Weinzierl, *Fast evolution of parton distributions*, *Comput. Phys. Commun.* **148** (2002) 314–326, [hep-ph/0203112].

[52] M. B. Hecht, C. D. Roberts, and S. M. Schmidt, *Valence-quark distributions in the pion*, *Phys. Rev.* **C63** (2001) 025213, [nucl-th/0008049].

[53] K. Wijesooriya, P. E. Reimer, and R. J. Holt, *The pion parton distribution function in the valence region*, *Phys. Rev.* **C72** (2005) 065203, [nucl-ex/0509012].